International Journal of Scientific & Engineering Research, Volume 10, Issue 2, February-2019
ISSN 2229-5518

Seasonal Rainfall Forecasting for Sinai Peninsula in Egypt Using Artificial Neural Networks

Hadeer E. Khafagy, Mohamed H. Elsanabary, Sherif E. Abdellah

Abstract— providing a forecasting tool for rainfall over Sinai Peninsula in Egypt will contribute in taking proper precautions for flash floods and eliminate their impacts as a result, so we employed the Artificial Neural Networks (ANN) for seasonal rainfall forecasting over Sinai Peninsula. This study forecasted the seasonal rainfall over El-Arish and Wadi Watir which are situated in Sinai Peninsula as two study cases using El-Nino southern oscillations (ENSO) seasonal data with a 3-month lead time. Moreover, the coefficient of determination (R^2) and the root mean square error (RMSE) were used to evaluate the forecasted rainfall values during both calibration and validation stages with the observed ones. During the calibration stage, (0.38 & 0.42 and 0.85 & 0.79) and (0.37 & 0.0.24 and 0.82 & 0.95) were the values of RMSE and R^2 while during the validation stage, RMSE and R^2 were found to be (0.09 & 0.25 and 0.89 & 0.92) and (0.52 & 0.13 and 0.71 & 0.97) For (El Arish) and (Wadi Watir), respectively for two study seasons. A comparison between rainfall data from in-situation measurements, satellite-estimated data from the previous studies and the forecasted rainfall resulted from this study showed that the ANN model was the most efficient among the available presented tools.

Index Terms— Sinai, Artificial Neural Networks, Feed-forward back-propagation, El-Arish Flash floods, Wadi Watir Flash floods, ENSO, Rainfall forecasting.

1 INTRODUCTION

Intensive rainfall is considered as one of the main severe climate events in hilly and rugged regions, such as Sinai Peninsula in Egypt, which has an inefficient drainage system (Ayoubi et al., 2018). Intensive rainfall events can lead to destructive flash floods causing massive damages to life and infrastructure (Yang et al., 2003). During the last three decades, Sinai Peninsula was affected by flash floods, For example, the flash flood event in January 2010. The 2010 flash flood drove six victims, dozens of injured, many missing, 592 fully destroyed houses,1487 partially devastated houses, the water level reached 2 m above the surface of the ground and the water demolished cars, trucks, trees, roads and communication lines (BBC News, January 18, 2010). Therefore, rainfall forecasting model can provide an early warning of flash flood events over Sinai Peninsula and consequently reduce the impact of flash flood events.

Considering the non-stationary characteristics of rainfall data, we used a non- stationary technique to describe and forecast a time series of rainfall data (Zhang, 2003). Artificial Neural Networks (ANN) is one of enormous non-linear structures which can be effective for processing such non-linear rainfall data (Arulsudar et al., 2005). Chibanga et al. (2003) presented a comparison of the ANN method with other statistical models which prove the ANN efficiency. The ANN feed-forward back-propagation trained method (used in this study) was effectively applied in resolving complex relationships, such as rainfall-runoff processes (Hsu et al., 2002; Chibanga et al., 2003; Srinivasulu & Jain, 2006 and Machado et al., 2011). Moreover, the ANN method was also involved in inflow forecasting of a reservoir (Shourian et al., 2008; Kim et al., 2009; Neelakantan & Pundarikanthan, 2000; Chiamsathit et al., 2016) and the evaluation for rainfall forecasting (Bodri & Cermak, 2000; and Bodri & Cermak 2001). Ferraris et al. (2002) also used the ANN technique to forecast the November 1994 flash flood in Northern Mediterranean.

In this study, El-Arish and Wadi Watir are considered as two study cases which are located in Sinai Peninsula. Cools et al. (2012) presented an early warning system (EWS) for flash floods over Wadi Watir in Sinai Peninsula. In addition, Cools et al. (2012) also analyzed the January 18, 2010 flash flood over Wadi Watir. Table 1 displayed flash flood events history and volume over Wadi Watir from 1987-2008 as Eissa et al. (2013) provided. El-Arish was subjected to a flash flood in January 2010 with a strength that had not been noticed in Sinai since 1980 (Moawad, 2013). Moreover, one of the flash flood events that were recorded during the study period (1981-2015) over El-Arish occurred on November, 1994, as mentioned by (Moawad, 2013).

This study employed the ANN model using El Niño southern oscillations (ENSO) to forecast the seasonal rainfall over El-Arish and Wadi Watir from 1981 to 2015. The ANN models in this study were trained by a feed-forward backpropagation learning algorithm. This study had two objectives. First, generating ANN models to forecast Sinai rainfall (represented in El-Arish and Wadi Watir as two study cases) during two rainy seasons (the January, February and March (JFM) season and the October, November and December (OND) season) using a 3-month lead time of ENSO. This study evaluated the forecasted rainfall during both ANN calibration and validation

- *Hadeer E. Khafagy, Graduate Student, Port Said University, Civil Engineering Department, Port Fouad, Port Said 42523, Egypt, Hadeerelsayed2014@gmail.com*
- *Mohamed H. Elsanabary, Assistant Professor, Port Said University, Civil Engineering Department, Port Fouad, Port Said 42523, Egypt, mohamed.elsanabary@eng.psu.edu.eg*
- *Sherif E. Abdellah, Associate Professor, Port Said University, Civil Engineering Department, Port Fouad, Port Said 42523, Egypt, sherif.elsayed@eng.psu.edu.eg*

International Journal of Scientific & Engineering Research, Volume 10, Issue 2, February-2019
ISSN 2229-5518

stages with the observed data. Second, forecasting rainfall over El-Arish and Wadi Watir during the two study seasons for 2016, 2017 and 2018 using the generated ANN models.

TABLE 1
HISTORICAL RECORDS OF FLASH FLOODS OVER WADI WATIR FROM 1987-2008 (EISSA ET AL., 2013).

Flood Date	Volume (10^6 m^3)	Flash flood magnitude	Remarks
Oct-16-1987	45	Very High	Disaster
Dec-20-1987	--	Low	--
Oct-16-1988	15	High	Catchment outlet
Mar-12-1990	--	Low	--
Oct-20-1990	35	High	Catchment outlet
Mar-22-1991	--	Moderate	--
Mar-1993	--	High	Catchment outlet
Oct-1993	--	High	Catchment outlet
Jan-1-1994	--	Moderate	Catchment outlet
Nov-2-1994	--	Moderate	--
Nov-17-1996	--	Moderate	--
Jan-14-1997	--	Moderate	--
Oct-18-1997	--	Very High	Disaster
Jan-15-2000	--	Low	--
Dec-9-2000	--	Low	--
Oct-(27-31)-2002	--	Moderate	--
Nov-3-2002	--	Low	--
Dec-15-2003	--	Low	--
Feb-5-2004	--	Low	--
Oct-29-2004	--	Low	--
Oct-24-2008	--	Low	--

* -- No data

2 DESCRIPTION OF STUDY AREA

Sinai Peninsula is the north-eastern extremity of Egypt occupying an area of about 60,000 km2, about 6% of Egypt's total area, between longitudes 32°20′–34°52′ E and latitudes 27°45′–31°10′ N; refer to Fig.1 (Elewa &Qaddah, 2011). There are two main rainy seasons in Sinai: January, February and March (JFM) season; and October, November and December (OND) season. This study defined El-Arish city and Wadi Watir as two study cases representing Northern and southern Sinai, respectively. The study areas are situated in the semi-arid belt where the annual rainfall value is less than 100 mm/year.

El-Arish is located in Sinai Peninsula between 31° 12′ 29.63″, 30° 57′ 59.18″ N and 33° 40′ 56.08″, 33° 58′ 7.98″ E which is the capital of Northern Sinai governorate, refer to Fig.1. It is situated 344 km northeast of Cairo. It is the largest city in the peninsula with an area of about 570 km2. El-Arish population is counted as 164,830 inhabitants in 2012. Rain cultivating is an essential activity for El-Arish residents (El Alfy, 2012).

Wadi Watir in Fig.1 is located in Southern Sinai between longitude 34° 38′ and 34° 41′ E and latitude 28° 57′ and 29° 03′ N in the southeastern portion of Sinai Peninsula, Egypt (Eisa et al., 2013) with an area of 3580 km2 (Cools et al., 2012). El-Arish and Wadi Watir as a part of Sinai were subjected to frequent flash flood events leading to enormous losses during the study period from 1981 to 2015 (Cools et al., 2012). Table 1 demonstrated the historical data of flash floods that hit Wadi Watir region.

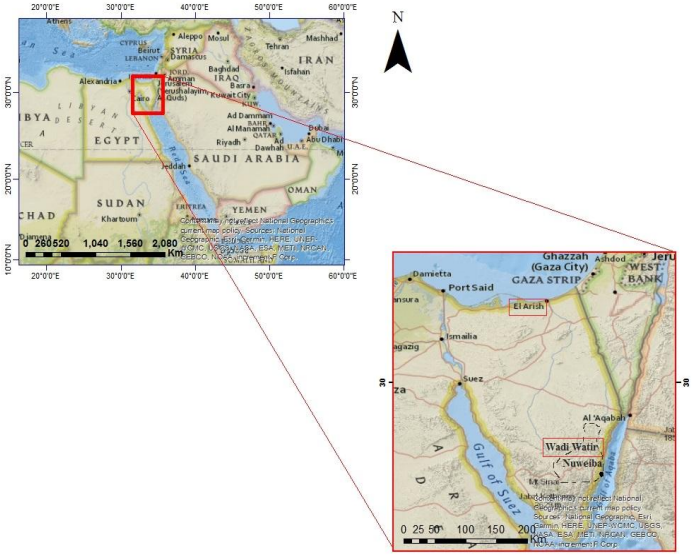

Fig.1: Arc GIS maps showing the location of El-Arish and Wadi Watir, Sinai, Egypt. Maps sources are: National Geographic, Esri, Garmin, HERE, UNEP-WCMC, USGS, NASA, ESA, METI, NRCAN, GEBCO, NOAA, and increment P Corp.

3 DATA

Data were collected from the European Center for Medium-Range Weather Forecasts (ECWMF) ERA-Interim dataset website at (http://apps.ecmwf.int/datasets/data/interim-mdfa/levtype=sfc/?). This data covered El-Arish city over 31° N, 33.50° E and Wadi Watir over 34.25 – 34.5° E, 28.5 – 29.25° N with a grid resolution of 0.25° x 0.25°. El-Arish and Wadi Watir rainfall data were collected for January, February, March, October, November and December every year from 1981 to 2015. Rainfall data were monthly means of daily accumulations. Rainfall values for Wadi Watir grid points were collected and normalized to get the mean values. After that, the average values were calculated for El-Arish and Wadi Watir to acquire January, February and March (JFM) and October, November and December (OND) seasonal means values.

Seasonal ERSSTv5 Niño 3.4 data at 5oNorth-5oSouth and 170-120oWest were downloaded from climate prediction centre of National Oceanic and Atmospheric Administration (NOAA) (Retrieved from: http://www.cpc.ncep.noaa.gov/data/indices/oni.ascii.txt) for the period 1981-2018.

4 METHODOLOGY

4.1 Artificial Neural Network Model

Artificial Neural Networks (ANN) is a model for data processing based on the characteristics of biological neural systems. It deals with and adapts complex and non-linear data similarly to the human brain. Researchers widely performed the ANN because of its accuracy and its ability to create complex non-linear models, especially in the field of climate and

International Journal of Scientific & Engineering Research, Volume 10, Issue 2, February-2019
ISSN 2229-5518

water resources (Suparta & Alhasa, 2016). The model consists of three layers which are: input, hidden and output, as demonstrated in Fig.2 (Machado et al., 2011). An ANN consists of elements called neurons linked with each other by connections called links and each link has its own weight parameter (Chen, 2016). Neurons can receive stimulus from outside the network. In this case, they are called input neurons. Neurons can also receive stimulus from other neurons in the network, they are called hidden neurons. There are many types of ANN which can be determined by the way of the neuron to connect and the data to process by a neuron (Zhang & Gupta, 2000). Suparta & Alhasa (2016) already explained types and methods of the ANN model. This study applied the feed-forward back-propagation Levenberg-Maquardt method.
In the ANN feed-forward, the data flows only in the forward direction. For a specific connection in the input layer, inputs are multiplied by the weights. Each neuron in the hidden layer receives a linear collection of the input elements. This collection produces a stimulus to the transfer function that delivers an output. Inputs to the next layer are the responses of the transfer functions. The input to the output layer is the linear collection of the outputs from the hidden layer. The output from the output layer is ANN response (Arulsudar et al., 2005). Equation (1) states mathematically the output from the three layers of ANN.

$$x = \beta\left(\sum_{i=1}^{r} m_{ni}\, \beta\left(\sum_{j=1}^{s} m_{ij} y_j + a_i\right) + a\right) \quad (1)$$

Assume y is the input elements, m is the weights between the connections, a is the biases, s is the number of neurons in the input layer, r is the number of neurons in the hidden layer, β is the transfer function, x is the ANN output and j, i and n are neurons of the input, respectively hidden and output layers. The vector of inputs y is fitted to be a vector of outputs P using the regression function of $f(y, m)$. Therefore, the function of $f(y, m)$ contains a family of curves and the object is to obtain the curve which will improve the performance. Choosing an ANN model to solve a problem depends on the choice of the functional form of $f(y, m)$ and estimating the weights vector m. The ANN model is summarized in three steps, which are: selection, calibration and validation.

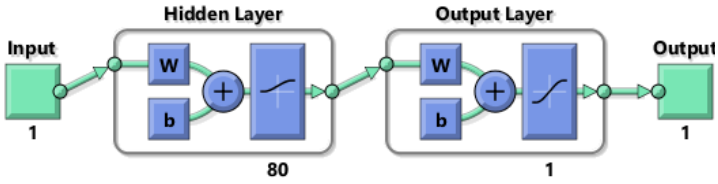

Fig.2: The feed forward back-propagation ANN network structure used in the study (Matlab figure).

4.1.1 Selection Stage

Modelling process of ANN based on the try and error method basically. In order to obtain an accurate ANN model, suitable input variables were determined. Moreover, the number of neurons in the three layers (input, hidden and output) was selected by trial and error.

4.1.2 Calibration (Training) Stage

Training is a search operation for the perfect set of weight values (Aytek et al., 2008). Picking out convenient training procedures can lead to efficient forecasted results with a good coherence to the observed data (Cigizoglu, 2003). The perfect chosen set can minimize the error between the simulation and experimental data in the output layer (Arulsudar et al., 2005). The number of times the ANN was trained is the number of iterations to determine weights and biases (Machado et al., 2011). Several ANN architectures for El-Arish and Wadi Watir were tested to obtain the convenient architecture. The Levenberg-Maquardt is the method used for training the ANN model in this study.
Levenberg-Maquardt, which is represented by equation (2), is an expansion of the Newton-Raphson method (Machado et al., 2011). Where the Newton-Raphson method assumed an objective quadratic function represented in the form of equation (3).

$$\Delta m\_in = -(\sigma(\theta \mid m\_in))/(Z\_\theta \mid m\_in) \quad (2)$$

While $(z_\theta|m_{in})$ is the Hessian matrix of the objective function, $(\theta|m_{in})$ is the gradient of the objective function (Aksoy & Dahamsheh, 2009).

$$\theta(c) = \sum^{c}{}_{=1}[e\ (c)]^2 \quad (3)$$

While $e_n(c)$ is the error between the observed output and the output forecasted by the model in the output layer, c is the length of the data series.
Machado et al. (2011) suggested computing the corrections of the weights and biases by assuming that L is the Jacobian matrix containing the derivatives of the error function with respect to the weights. $\rho > 0$ is a parameter, and T denotes the transpose of a matrix so that equation (2) will be as equation (4).

$$\Delta m_{in} = -[L^T(n)\, L(n) + \rho h]^{-1}\, L^T(n)\, e(n) \quad (4)$$

4.1.3 Validation (Testing) Stage

In the validation stage, the selected model in the previous calibration stage was tested by training using the rest 6 years of data from 2010-2015 which were not involved in the calibration stage. In order to make sure the calibrated model is reliable, the validated ANN model performance was compared to the calibrated one (Elsanabary & Gan, 2015). The determination of the final optimal model for forecasting depends on its high performance. Generally, the decision of choosing the convenient model is dependent on the values of the root mean square error (RMSE) and the determination coefficient (R2) values which can be calculated as follows:

$$RMSE = \sqrt{\frac{\sum_{j=1}^{b} R_{f,j} - R_{i,j})^2}{b}} \quad (5)$$

International Journal of Scientific & Engineering Research, Volume 10, Issue 2, February-2019
ISSN 2229-5518

$$R^2 = \frac{\sum_{j=1}^{b}\left(R_{f,j}-\bar{R}_f\right)\left(R_{i,j}-\bar{R}_i\right)}{\sqrt{\sum_{j=1}^{b}\left(R_{f,j}-\bar{R}_f\right)}\sqrt{\sum_{j=1}^{b}\left(R_{i,j}-\bar{R}_i\right)}} \quad (6)$$

Where $R_{f,j}$ and $R_{i,j}$ represent respectively the observed and the forecasted rainfall, b is the total number of data points, and $\bar{R}_f$ & $\bar{R}_i$ correspond to the mean of the observed and the forecasted rainfall (Cigizoglu, 2003). Minimum RMSE and maximum $R^2$are obtained when selecting an ANN model with high performance. Model performance can be improved by increasing the length of the data series or increasing number of neurons in the hidden layer (Zhang, 2003).

5 Results and Discussions

5.1 Forecasting of El-Arish and Wadi Watir rainfall using ENSO data as predictors

This study applied the feed-forward back-propagation ANN technique to forecast seasonal rainfall of two study areas, El-Arish and Wadi Watir. The network architecture for all models consists of an input layer with one neuron, an output layer with one neuron and a hidden layer with 80 neurons for all selected ANN models. Generally, input data of ENSO and output data of El-Arish and Wadi Watir seasonal rainfall were normalized by subtracting the mean and dividing into square variance before the ANN analysis. The ANN model was first calibrated using 29 years (1981-2009) of data then it independently validated using the rest 6 years of data (2010-2015). The model was still calibrated until a high-performance model with low RMSE value and high R2 value was obtained. When the appropriate model selected in the calibration stage, the values of R2 and RMSE assured in the next validation stage and may become higher. The period of three months as a forecasting lead time is a sufficient period for taking proper precautions to avoid flash floods impacts. Therefore, the model is further simulated using ENSO OND data to obtain the forecasted values of El-Arish and Wadi Watir rainfall within the JFM season. The forecasted rainfall values which were obtained after both the calibration and validation stages were separately evaluated with the observed values of El-Arish and Wadi Watir JFM and the time series plotted in Fig.3 and Fig.4, respectively. Using ENSO July, August and September (JAS) data as predictors, the same steps were repeated and the forecasted rainfall evaluations with the observed data were obtained for El-Arish and Wadi Watir during the OND season. The forecasted and observed rainfall data during the OND season were presented in Fig.5 and Fig.6, respectively. The values of RMSE and R2 for El-Arish and Wadi Watir during the JFM and the OND seasons of the selected models were concluded in Tables 2 and 3, respectively.

TABLE 2
THE PROPERTIES OF APPLIED ANN MODELS USED IN FORECASTING EL-ARISH RAINFALL DATA DURING THE JFM AND THE OND SEASON.

		El Arish					
Season	Input Data	Output Data	Stage	Data Period	Number of Neurons	RMSE	R^2
JFM	ENSO OND	El-Arish JFM rainfall data	Calibration	1981-2009	80 neurons	0.38	0.85
			Validation	2010-2015		0.09	0.89
			Forecasting	2016-2018		Mean= 0.47	Mean= 0.87
OND	ENSO JAS	El-Arish OND rainfall data	Calibration	1981-2009		0.42	0.79
			Validation	2010-2015		0.25	0.92
			Forecasting	2016-2017		Mean= 0.34	Mean= 0.86

TABLE 3
THE PROPERTIES OF APPLIED ANN MODELS USED IN FORECASTING WADI WATIR RAINFALL DATA DURING THE JFM AND THE OND SEASON.

		Wadi Watir					
Season	Input Data	Output Data	Stage	Data Period	Number of Neurons	RMSE	R^2
JFM	ENSO OND	Wadi Watir JFM rainfall data	Calibration	1981-2009	80 neurons	0.37	0.82
			Validation	2010-2015		0.52	0.71
			Forecasting	2016-2018		Mean= 0.45	Mean= 0.77
OND	ENSO JAS	Wadi Watir OND rainfall data	Calibration	1981-2009		0.24	0.95
			Validation	2010-2015		0.13	0.97
			Forecasting	2016-2017		Mean= 0.37	Mean= 0.96

Fig.3, Fig.4, Fig.5 and Fig.6 exhibited the time series of the observed and the forecasted rainfall after both the calibration and validation stages using the ANN models of El-Arish and Wadi Watir during the JFM and the OND seasons from 1981 to 2018. The two plotted time series of observed and forecasted rainfall were compared considering the high value of the standard precipitation is an indication of flash flood existence. Consequently, Fig.3 confirmed that the generated ANN model efficiently forecasted the flash flood event which occurred in 2010 over El-Arish during the JFM season. Fig.4 affirmed that the generated ANN model could efficiently forecast the flash flood event that occurred in 1994 over El-Arish during the OND season. Furthermore, Fig.5 assured that the generated ANN model efficiently forecasted the flash flood events that occurred in 1990, 1991, 1993, 1994, 1997 and 2000 over Wadi Watir during the JFM season. Otherwise, the model failed to forecast only the flash flood event that occurred in 2004 over Wadi Watir. Moreover, Fig.6 assured that the generated ANN model efficiently forecasted the flash flood events that occurred in 1987, 1988, 1990, 1993, 1994, 1997, 2000, 2002, 2003, 2004 and 2008 over Wadi Watir during the OND season. However, the ANN model successfully indicated to the flash flood event that occurred in 1996 over Wadi Watir, the satellite-estimated data represented in ERA-Interim data, used in this study, failed to measure the observed rainfall volume produced due to the event. Cools et al. (2012) mentioned that the satellite-estimated rainfall, such as ERA-Interim data, capture only the regional events and can miss the local events.

Cools et al., (2012) provided rainfall data obtained over Wadi Watir for flash flood events from 2002-2010 using three

International Journal of Scientific & Engineering Research, Volume 10, Issue 2, February-2019
ISSN 2229-5518

different sources: in-situ measurements, Weather Research and Forecasting (WRF) tool, and satellite-estimated data by visualization tool of Tropical Rainfall Measuring Mission (TRMM). Therefore, the ANN forecasted rainfall values for the flash flood events since 2002 which resulted in this study were compared to the values mentioned by Cools et al. (2012) and listed in Table 4. The WRF successfully forecasted 6 of total 7 events since 2002 while the 2002 event is a non-forecasted event. Furthermore, the TRMM failed to forecast 4 events out of 7 events including the 2008 flash flood event, while the in-situ measurements data were obtainable for 4 out of 7 events, including the flash flood events in October 2008 and January 2010. Generally, ANN models effectively forecasted almost all events since 2002, whereas the ANN model failed to indicate only the flash flood event that occurred on 2004 over Wadi Watir.

This study employed the resulted ANN models to forecast the seasonal rainfall over El-Arish and Wadi Watir within the JFM season for 2016-2018 and the OND season for 2016-2017 after the study period from 1981-2015. The time series of the forecasted rainfall values over El-Arish and Wadi Watir within the JFM and OND seasons were presented in Fig.3, Fig.4, Fig.5 and Fig.6.

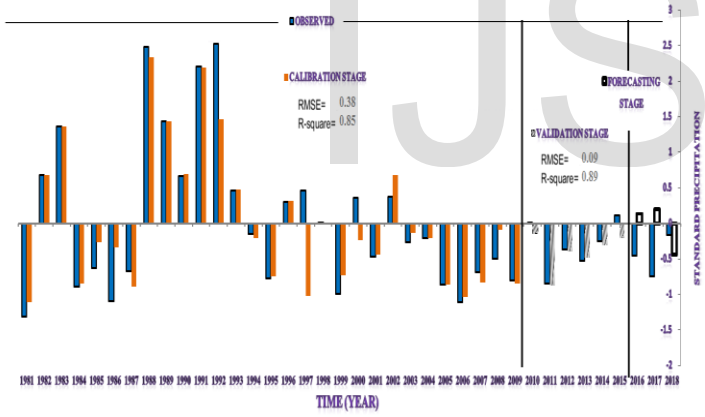

Fig.3: Observed and forecasted (resulted) rainfall evaluation after both the calibration and validation stages of El-Arish during the JFM season from 1981-2015 and forecasted rainfall from 2016-2018.

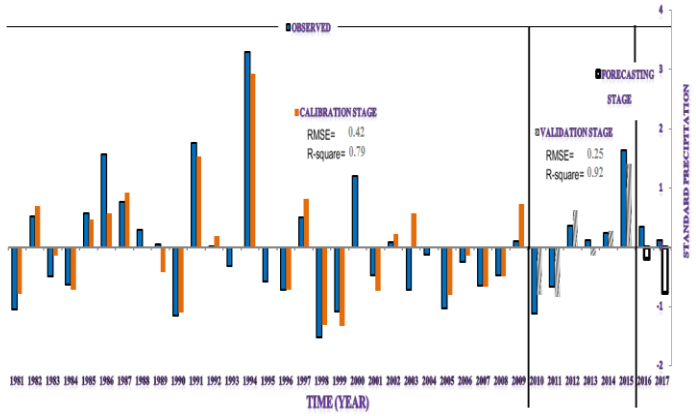

Fig.4: Observed and forecasted (resulted) rainfall evaluation after both the calibration and validation stages of El-Arish during the OND season from 1981-2015 and forecasted rainfall from 2016-2017.

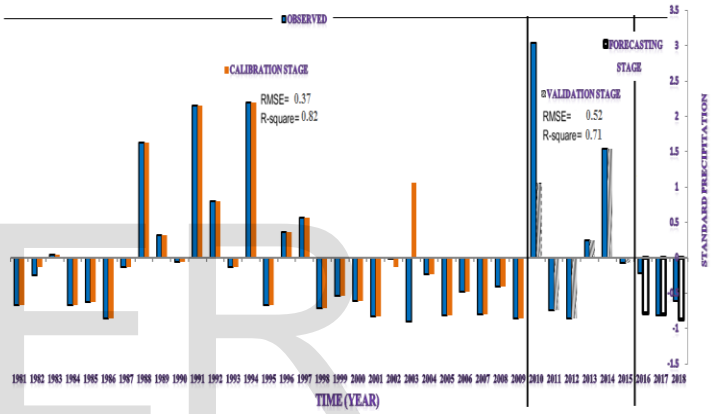

Fig.5: Observed and forecasted (resulted) rainfall evaluation after both the calibration and validation stages of Wadi Watir during the JFM season from 1981-2015 and forecasted rainfall from 2016-2018.

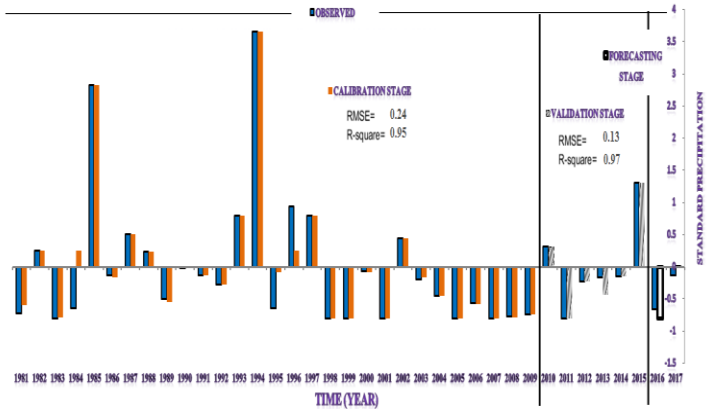

Fig.6: Observed and forecasted (resulted) rainfall evaluation after both the calibration and validation stages of Wadi Watir during the OND season from 1981-2015 and forecasted rainfall from 2016-2017.

International Journal of Scientific & Engineering Research, Volume 10, Issue 2, February-2019
ISSN 2229-5518

TABLE 4
QUALITATIVE COMPARISON OF THE AVAILABLE RAINFALL DATA OVER WADI WATIR RESULTED FROM ANN FORECASTS, IN-SITU MEASUREMENTS, WRF FORECASTS, AND SATELLITE ESTIMATES (TRMM) FOR FLASH FLOODS FROM 2002-2010 (COOLS ET AL., 2012).

Max. cumulative rainfall (mm)					
Date	Flash flood Magnitude	ANN rainfall forecast	TRMM estimate	WRF rainfall forecast	in-situ observations (mm)
30 Oct 2002	Moderate	Moderate	10	--	9
15 Dec 2003	---	Moderate	--	36	--
5 Feb 2004	---	Moderate	--	13.5	8
29 Oct 2004	Weak	Weak	12	5	--
28 Mar 2006	---	Weak	--	14	--
23–24 Oct 2008	Moderate	Weak	2.5	2	0.3-11
17–18 Jan 2010	High	Moderate	30.5	36	11-30

6 SUMMARY AND CONCLUSIONS

ENSO data with a 3-month lead time were used to generate Artificial Neural Networks (ANN) models to forecast El-Arish and Wadi Watir seasonal rainfall. The forecasted values evaluated with the observed data for both study cases within the two seasons (JFM and OND). For El-Arish and Wadi Watir, the mean values of RMSE and R2 during the two stages (calibration and validation) were (0.47 & 0.87 and 0.45 and 0.77) and (0.34 & 0.86 and 0.37 & 0.96) within the (JFM) and the (OND) seasons, respectively.

This study employed ENSO data from 2016-2018 (after the period which was involved in the calibration and validation stages of the model) to forecast rainfall over the two study cases during the JFM and OND seasons from 2016-2018. According to this study, the ANN models effectively forecasted all recorded events since 2002 over Wadi Watir except the flash flood on February 5, 2004, so that the ANN model is the most efficient among the available measurement techniques that presented in the previous studies.

Water from flash floods can be stored and exploited as one of the water resources. Thus, rainfall forecasting is important to the management of water resources in Sinai. Furthermore, flash flood forecasting can reduce their impacts by taking the proper precautions. This study will assist Sinai's Bedouins to get sustainable sources of water and the government to prevent the negative impacts of flash flood events and water shortage.

6.1 Recommendations for Future Work

Dataset expansion upgrades the forecasting accuracy using the ANN model, so studies should be carried out to extend the training dataset of the ANN model. Otherwise, future studies can be incorporated into this study to determine a potential location for reservoirs construction in the future in order to save rainwater. Reliable forecasted rainfall values are essential for determining the design dimensions of such hydraulic structures.

ACKNOWLEDGMENT

This research did not receive any specific grant from funding agencies in the public, commercial, or not-for-profit sectors. Rainfall data were provided by the European Centre for Medium-Range Weather Forecasts (ECWMF) ERA-Interim dataset at (http://apps.ecmwf.int/datasets/data/interim-mdfa/levtype=sfc/?). Data of El Niño 3.4 were downloaded from climate prediction center of the National Oceanic and Atmospheric Administration (NOAA) at (http://www.cpc.ncep.noaa.gov/data/indices/oni.ascii.txt). All captions for the entire tables do not need footnote letters.

REFERENCES

[1] Aksoy, H., & Dahamsheh, A. (2009). Artificial neural network models for forecasting monthly precipitation in Jordan. Stoch Environ Res Risk. doi:10.1007/s00477-008-0267-x.

[2] Arulsudar, N., Subramanian, N., & Murthy, R. S. (2005). Comparison of artificial neural network and multiple linear regression in the optimization of formulation parameters of leuprolide acetate loaded liposomes. J Pharm Pharmaceut Sci. Retrieved from www. cspsCanada.org.

[3] Ayoubi, S., Mokhtari, J., Mosaddeghi, M.R. & Zeraatpisheh, M. (2018). Erodibility of calcareous soils as influenced by land use and intrinsic soil properties in a semiarid region of central Iran. Environmental monitoring and assessment, 190, 192.

[4] Aytek, A., Guven, A., Yuce, M. I., & Aksoy, H. (2008). An explicit neural network formulation for evapotranspiration. Hydrological Sciences Journal, 53(4), 893-904. doi:10.1623/hysj.53.4.893

[5] BBC News. Flash floods in Egypt and Israel kill seven. (2010, January 18). From http://news.bbc.co.uk/2/hi/middle_east/8466546.stm. Retrieved on 18/12/2017.

[6] Bodri L. & Cermak V. (2000). Prediction of extreme precipitation using a neural network: application to summer flood occurrence in Moravia. Adv Eng Softw 31:311–321

[7] Bodri L. & Cermak V. (2001). Neural network prediction of monthly precipitation: application to summer flood occurrence in two regions of central Europe. Studia Geoph et Geod 45:155–167

[8] Chen, M. (2016). Use of Artificial Neural Network for Land Use La nd Cover Classification of UAV Acquired Imagery. Thesis Submitted to Symbiosis Institute of Geoinformatics, Symbiosis International University. Retrieved from https://www.sig.ac.in/assets/student_proect_pdf/MarciaChenThesis.pdf.

[9] Chiamsathit, C., Adeloye, A. J., & Bankaru-Swamy, S. (2016). Inflow forecasting using Artificial Neural Networks for reservoir operation. Proceedings of the International Association of Hydrological Sciences, 373, 209-214. doi:10.5194/piahs-373-209-2016.

[10] Chibanga, R., Berlamont, J., & Vandewalle, J. (2003). Modelling and forecasting of hydrological variables using artificial neural networks: The Kafue River sub-basin. Hydrological Sciences Journal, 48(3), 363-379. doi:10.1623/hysj.48.3.363.45282.

[11] Cigizoglu, H. K. (2003). Incorporation of ARMA models into flow forecasting by artificial neural networks. Environmetrics, 14(4), 417-427. doi:10.1002/env.596.

[12] Climate Prediction Center. Accessed February 18, 2017.

International Journal of Scientific & Engineering Research, Volume 10, Issue 2, February-2019
ISSN 2229-5518

http://www.cpc.ncep.noaa.gov/data/indices/oni.ascii.txt.

[13] Cools, J., Vanderkimpen, P., El Afandi, G., Abdelkhalek, A., Fockedey, S., El Sammany, M., and Huygens, M. (2012). An early warning system for flash floods in hyper-arid Egypt. Natural Hazards and Earth System Sciences. doi:10.5194/nhess-12-443-2012

[14] Eissa, M. A., Thomas, J. M., Pohll, G., Hershey, R. L., Dahab, K. A., Dawoud, M. I., and Gomaa, M. A. (2013). Groundwater resource sustainability in the Wadi Watir delta, Gulf of Aqaba, Sinai, Egypt. Hydrogeology Journal, 21(8), 1833-1851. doi:10.1007/s10040-013-1031-y.

[15] El Alfy, M., (2012). Integrated geostatistics and GIS techniques for assessing groundwater contamination in Al Arish area, Sinai, Egypt. Arab J Geosci. DOI 10.1007/s12517-010-0153-y.

[16] Elewa H. H., & Qaddah A. A. (2011). Ground water potentiality mapping in the Sinai Peninsula, Egypt, using remote sensing and GIS-watershed-based modeling. Hydrogeology Journal.

[17] Elsanabary, M. H., & Gan, T. Y. (2015). Weekly Streamflow Forecasting Using a Statistical Disaggregation Model for the Upper Blue Nile Basin, Ethiopia. Journal of Hydrologic Engineering, 20(5), 04014064. doi:10.1061/(asce)he.1943-5584.0001072.

[18] ERA-Interim, Monthly Means of Daily Forecast Accumulations. Accessed February 09, 2017. http://apps.ecmwf.int/datasets/data/interim-mdfa/levtype=sfc/.

[19] Ferraris, L., Rudari, R., & Siccardi, F. (2002). The Uncertainty in the Prediction of Flash Floods in the Northern Mediterranean Environment. Journal of Hydrometeorology, 3(6), 714-727. doi:10.1175/1525-7541(2002)0032.0.co;2.

[20] Hsu, K., Gupta, H. V., Gao, X., Sorooshian, S., & Imam, B. (2002). Self-organizing linear output map (SOLO): An artificial neural network suitable for hydrologic modeling and analysis. Water Resources Research, 38(12). doi:10.1029/2001wr000795.

[21] Kim, T., Choi, G., & Heo, J. (2009). Inflow Forecasting for Real-Time Reservoir Operation Using Artificial Neural Network. World Environmental and Water Resources Congress 2009. doi:10.1061/41036(342)499.

[22] Machado, F., Mine, M., Kaviski, E., & Fill, H. (2011). Monthly rainfall–runoff modelling using artificial neural networks. Hydrological Sciences Journal. Retrieved April, 2018, from https://www.tandfonline.com/doi/abs/10.1080/02626667.2011.559949#aHR0cHM6Ly93d3cudGFuZGZvbmxpbmUuY29tL2RvaS9wZGYvMTAuMTA4MC8wMjYyNjY2Ny4yMDExLjU1OTk0OT9uZWVkQWNjZXNzPXRydWVAQEAw

[23] Moawad, M. B. (2013). Analysis of the flash flood occurred on 18 January 2010 in wadi El Arish, Egypt (a case study). Geomatics, Natural Hazards and Risk, 4(3), 254-274. doi:10.1080/19475705.2012.731657.

[24] Neelakantan, T. R., & Pundarikanthan, N. V. (2000). Neural Network-Based Simulation-Optimization Model for Reservoir Operation. Journal of Water Resources Planning and Management, 126(2). Retrieved April 11, 2018, from https://ascelibrary.org/doi/pdf/10.1061/(ASCE)0733-9496(2000)126:2(57).

[25] Shourian, M., Mousavi, S. J., Menhaj, M. B., & Jabbari, E. (2008). Neural-network-based simulation-optimization model for water allocation planning at basin scale. Journal of Hydroinformatics, 10(4), 331. doi:10.2166/hydro.2008.057.

[26] Srinivasulu, S., & Jain, A. (2006). A comparative analysis of training methods for artificial neural network rainfall–runoff models. Applied Soft Computing, 6(3), 295-306. doi:10.1016/j.asoc.2005.02.002

[27] Suparta, W., & Alhasa, K. M. (2016). Adaptive Neuro-Fuzzy Interference System. In Modeling of tropospheric delays using ANFIS. Cham: Springer.

[28] Yang, D., Kanae, S., Oki, T., Koike, T., & Musiake, K. (2003). Global potential soil erosion with reference to land use and climate changes. Hydrological Processes, 17(14), 2913-2928. doi:10.1002/hyp.1441.

[29] Zhang, Q. J., & Gupta, K. C. (2000). Neural Network Structures. In Neural Networks for RF and Microwave Design. Boston: Artech House.

[30] Zhang, G. (2003). Time series forecasting using a hybrid ARIMA and neural network model. Neurocomputing, 50, 159-175. doi:10.1016/s0925-2312(01)00702-0

[31] H. Goto, Y. Hasegawa, and M. Tanaka, "Efficient Scheduling Focusing on the Duality of MPL Representation," Proc. IEEE Symp. Computational Intelligence in Scheduling (SCIS '07), pp. 57-64, Apr. 2007, doi:10.1109/SCIS.2007.367670. (Conference proceedings)

[32] J. Williams, "Narrow-Band Analyzer," PhD dissertation, Dept. of Electrical Eng., Harvard Univ., Cambridge, Mass., 1993. (Thesis or dissertation)

[33] E.E. Reber, R.L. Michell, and C.J. Carter, "Oxygen Absorption in the Earth's Atmosphere," Technical Report TR-0200 (420-46)-3, Aerospace Corp., Los Angeles, Calif., Nov. 1988. (Technical report with report number)

[34] L. Hubert and P. Arabie, "Comparing Partitions," J. Classification, vol. 2, no. 4, pp. 193-218, Apr. 1985. (Journal or magazine citation)

[35] R.J. Vidmar, "On the Use of Atmospheric Plasmas as Electromagnetic Reflectors," IEEE Trans. Plasma Science, vol. 21, no. 3, pp. 876-880, available at http://www.halcyon.com/pub/journals/21ps03-vidmar, Aug. 1992. (URL for Transaction, journal, or magzine)

[36] J.M.P. Martinez, R.B. Llavori, M.J.A. Cabo, and T.B. Pedersen, "Integrating Data Warehouses with Web Data: A Survey," IEEE Trans. Knowledge and Data Eng., preprint, 21 Dec. 2007, doi:10.1109/TKDE.2007.190746.(PrePrint)